AIAA JOURNAL
Vol. 37, No. 11, November 1999

Simulations of Reacting Droplets Dispersed in Isotropic Turbulence

Farzad Mashayek*
University of Hawaii at Manoa, Honolulu, Hawaii 96822

Several important issues pertaining to dispersion and polydispersity of evaporating and reacting fuel droplets in forced turbulent flows are investigated. The carrier phase is considered in the Eulerian context and is simulated by direct numerical simulation. The dispersed phase is tracked in the Lagrangian frame and the interactions between the phases are taken into account in a realistic two-way coupled formulation. It is assumed that combustion takes place in the vapor phase and is described as fuel + oxidizer $\longrightarrow$ products + energy. The resulting scheme is applied for extensive simulations of a forced, isotropic, low Mach number turbulent flow laden with a large number of fuel droplets. Here the results are presented for different values of the mass loading ratio and the heat release coefficient. The combustion process is significantly affected by the rate of evaporation and the fuel vapor participates in the chemical reaction almost immediately after its production. A strong correlation is observed between the droplet concentration and the reaction rate. The results are also used to discuss the temporal evolution of the mean temperatures and the mean mass fractions, as well as the role of the preferential distribution of the droplets.

Nomenclature

B = transfer number, $(T^* - T_d)/\lambda$
C = droplet concentration, $\sum^{n_d} m_d/(\rho\delta\mathcal{V})$
Ce = heat release coefficient, $[1/(\gamma-1)M_f^2][\lambda - (1+r)(h_p^f/C_pT_f)]$
C_p = specific heat of the carrier phase
Da = Damköhler number, $\rho_f L_f K_{\text{fwd}}/U_f$
d_d = droplet diameter
E_I = sensible internal energy of the carrier phase, $\rho C_v T$
E_K = kinetic energy of the carrier phase, $\frac{1}{2}\rho u_i u_i$
E_T = total energy of the carrier phase, $E_I + E_K$
$\mathcal{F}_i$ = zero-mean solenoidal random force
f_1 = $(1 + 0.15Re_d^{0.687})/(1+B)$
f_2 = $Nu/3\,Pr$
f_3 = $\rho^* Sh\lambda/3Sc$
f_4 = $\pi(18/\rho_d)^{0.5}(\rho^* Sh/Re_f^{1.5}Sc)$
h = specific enthalpy
h_p^f = enthalpy of formation of the product gas
K_{fwd} = forward reaction rate constant
k = wavenumber
L_f = reference length
L_v = latent heat of vaporization of the liquid
M_f = reference Mach number, $U_f/\sqrt{(\gamma RT_f)}$
m_d = mass of the droplet
N = number of collocation points in each direction
Nu = Nusselt number, $(2 + 0.6Re_d^{0.5}Pr^{0.33})/(1+B)$
N_d = total number of droplets
n_d = number of droplets within the cell volume
Pr = Prandtl number, $C_p\mu/\kappa$
p = pressure of the carrier phase
R = gas constant
Re_d = droplet Reynolds number, $Re_f\rho^* d_d|u_i^* - v_i|$
Re_f = reference Reynolds number, $\rho_f U_f L_f/\mu$
r = stoichiometric coefficient
Sc = Schmidt number, $\mu/\rho\Gamma$
Sh = Sherwood number, $2 + 0.6Re_d^{0.5}Sc^{0.33}$
S_{ij} = rate-of-strain tensor, $\frac{1}{2}(\partial u_i/\partial x_j + \partial u_j/\partial x_i)$
$\mathcal{S}_m, \mathcal{S}_{ui}, \mathcal{S}_e$ = coupling source/sink terms
T = temperature
T_B = boiling temperature of the liquid
t = time
U_f = reference velocity
u_i = velocity of the carrier phase in direction x_i $(i = 1, 2, 3)$
v_i = velocity of the droplet in the direction x_i
X_i = position of the droplet
x_i = spatial coordinates
Y_{fv} = fuel vapor mass fraction
Y_{ox} = oxidizer mass fraction
Γ = binary mass diffusivity coefficient
γ = ratio of the specific heats of the carrier gas
Δ = dilatation, $\partial u_j/\partial x_j$
$\delta\mathcal{V}$ = cell volume
δx = node spacing
δ_{ij} = Kronecker delta function
ϵ = dissipation rate
κ = thermal conductivity of the carrier phase
λ = normalized latent heat of evaporation, L_v/C_pT_f
μ = viscosity of the carrier phase
ξ = mixture fraction
ρ = density
τ_d = droplet time constant, $Re_f\rho_d d_d^2/18$
Φ_m = mass loading ratio
ω = reaction rate, $\rho^2 Da Y_{\text{fv}} Y_{\text{ox}}$

Subscripts

B = boiling condition
d = droplet properties
f = reference parameters for normalization
fv = fuel vapor
ox = oxidizer
s = surface of the droplet
0 = initial value at $t = 0$

Superscripts

$'$ = fluctuating quantity
$*$ = carrier phase properties at the droplet location

Received 24 August 1998; presented as Paper 99-0204 at the 37th Aerospace Sciences Meeting, Reno, NV, 11–14 January 1999; revision received 13 April 1999; accepted for publication 13 April 1999.

*Assistant Professor, Department of Mechanical Engineering, 2540 Dole Street. Senior Member AIAA.

Introduction

NUMERICAL simulation of turbulent reacting flows has proven to be one of the most challenging tasks within the general field of computational fluid dynamics.[1–3] Turbulent flows are exemplified

by their many length- and timescales that require high resolution and/or accurate modeling for their simulation. The addition of chemical reaction to these flows introduces a new set of variables often accompanied by sharp gradients in small scales. The complexity of the turbulent reacting flow is obviously escalated by the presence of liquid droplets (or solid particles). Because of its nature, the multiphase flow is best analyzed in the Lagrangian frame by tracking a large number of droplets.[4]

With the advent of supercomputers, it became possible to simulate turbulent reacting flows via direct numerical simulation (DNS) without resorting to any modeling.[2,5–14] DNS has also been used for simulations of turbulent flows laden with particles.[15–26] The extent of contributions is too large to be discussed here in detail; we refer to recent reviews.[27–29] Most of the previous studies have considered dispersion of solid particles only. Recently, Mashayek et al.[30] implemented DNS for the study of evaporating droplets in one-way coupling with an incompressible carrier phase. This study shows that, after an initial transient period, the droplet-size distribution becomes nearly Gaussian. This result is verified qualitatively at low mass loading ratios by Mashayek,[31,32] who considered the compressible flow with two-way coupling. The results in Refs. 31 and 32 also indicate that evaporation is significantly affected by two factors, i.e., the gradient of the fuel vapor concentration in the vicinity of the droplets and the heat transfer from the carrier phase to the dispersed phase.

In light of our previous studies, in this paper we extend the application of DNS to evaporating and reacting droplets dispersed in a compressible carrier phase. Because this is one of the early attempts in DNS of reacting droplet dispersion in turbulent flows with two-way coupling, the problem is formulated based on models and correlations that are relatively well established. It is also emphasized that the term DNS is used here with the understanding that there are models involved in describing the effects of the droplets on the carrier phase. Because of the presence of the droplets the flow is heterogeneous, whereas the combustion is assumed to take place in the vapor phase only, thus rendering a homogeneous reaction. For the range of the mass loading ratios considered, this assumption seems reasonable.[33] The investigation is based on the forced isotropic turbulent flow to avoid the extra complexity in the analysis of the results. This isotropic configuration (idealistically) resembles the flow in the combustion chamber of a gas turbine, provided sufficient distance from the walls. A large number of parameters emerge from the formulation of the problem. Although we have been able to perform extensive DNS to study the effects of many of these parameters, because of space limitation here we only consider the effects of the mass loading ratio and the heat release coefficient, analogous to Mashayek.[34] However, the formulation used here is slightly different and provides a higher resolution for the Eulerian fields, especially the carrier phase density. Also, all of the parameter values are the same as those in the cited study, except for the initial droplet time constant and the box Reynolds number. The droplet time constant in this study is chosen close to the carrier phase Kolmogorov timescale to magnify the effects of the preferential distribution.[18] Because the droplet size is larger, the evaporation rate is slower for the present simulations.

Formulation and Methodology

We consider the motion of a large number of fuel droplets (dispersed phase) in a turbulent flow (carrier phase). The transport of the carrier phase is considered in the Eulerian frame, whereas the dispersed phase is treated in a Lagrangian manner. Also, conservation equations (in the Eulerian frame) are considered for the mass fractions of the fuel vapor and the oxidizer. For simplicity, the fuel vapor, the oxidizer, and the products are assumed to have the same properties such that their mixture (hereinafter referred to as the carrier phase or the fluid) can be treated as one entity: the Eulerian continuity, momentum, and energy equations are solved for the mixture. The specific enthalpies of these components, however, are considered to be different to satisfy the first law of thermodynamics.

The carrier phase is considered to be a compressible and Newtonian fluid with zero bulk viscosity and to obey the perfect gas equation of state. The Eulerian forms of the nondimensional continuity, momentum, and energy equations for the carrier phase are expressed as

$$\frac{\partial \rho}{\partial t} + \frac{\partial}{\partial x_j}(\rho u_j) = \mathcal{S}_m \tag{1}$$

$$\frac{\partial}{\partial t}(\rho u_i) + \frac{\partial}{\partial x_j}(\rho u_i u_j) = -\frac{\partial p}{\partial x_i} + \frac{2}{Re_f}\frac{\partial}{\partial x_j}\left(S_{ij} - \frac{1}{3}\Delta\delta_{ij}\right) + \rho\mathcal{F}_i + \mathcal{S}_{ui} \tag{2}$$

$$\frac{\partial E_T}{\partial t} + \frac{\partial}{\partial x_j}[(E_T + p)u_j] = \frac{1}{(\gamma-1)PrRe_f M_f^2}\frac{\partial^2 T}{\partial x_j \partial x_j} + \frac{2}{Re_f}\frac{\partial}{\partial x_j}\left[u_i\left(S_{ij} - \frac{1}{3}\Delta\delta_{ij}\right)\right] + CeDa\rho^2 Y_{\mathrm{fv}} Y_{\mathrm{ox}} + \rho u_i \mathcal{F}_i + \mathcal{S}_e \tag{3}$$

followed by conservation equations for the fuel vapor and the oxidizer mass fractions:

$$\frac{\partial}{\partial t}(\rho Y_{\mathrm{fv}}) + \frac{\partial}{\partial x_j}(\rho Y_{\mathrm{fv}} u_j) = \frac{1}{ScRe_f}\frac{\partial^2 Y_{\mathrm{fv}}}{\partial x_j \partial x_j} - Da\rho^2 Y_{\mathrm{fv}} Y_{\mathrm{ox}} + \mathcal{S}_m \tag{4}$$

$$\frac{\partial}{\partial t}(\rho Y_{\mathrm{ox}}) + \frac{\partial}{\partial x_j}(\rho Y_{\mathrm{ox}} u_j) = \frac{1}{ScRe_f}\frac{\partial^2 Y_{\mathrm{ox}}}{\partial x_j \partial x_j} - rDa\rho^2 Y_{\mathrm{fv}} Y_{\mathrm{ox}} \tag{5}$$

The equation of state is $p = \rho T/\gamma M_f^2$. All of the variables are normalized by reference length, density, velocity, and temperature scales. The total energy equation [Eq. (3)] is derived by assuming unity Lewis number.[35] The coupling of the carrier phase with the droplets is through the terms $\mathcal{S}_m$, $\mathcal{S}_{ui}$, and $\mathcal{S}_e$ that, respectively, describe the mass, momentum, and energy exchange between the phases. The formulation of these terms and their calculation from the discrete droplet fields are described later in this section.

The liquid droplets are allowed to evaporate but are assumed to remain spherical with diameter smaller than the smallest length scale of the turbulence and to experience an empirically corrected Stokesian drag force. Both interior motions and rotation of the droplets are neglected. The density of the droplets is considered to be constant and much larger than the density of the carrier phase such that only the inertia and the drag forces are significant to the droplet dynamics. The droplet-droplet interaction and the radiation heat transfer are also neglected. The droplets are tracked individually in a Lagrangian manner, and the droplet position, velocity, temperature, and mass are determined from the following nondimensional equations[36]:

$$\frac{\mathrm{d}X_i}{\mathrm{d}t} = v_i \tag{6}$$

$$\frac{\mathrm{d}v_i}{\mathrm{d}t} = \frac{f_1}{\tau_d}(u_i^* - v_i) \tag{7}$$

$$\frac{\mathrm{d}T_d}{\mathrm{d}t} = \frac{f_2}{\tau_d}(T^* - T_d) - \frac{f_3}{\tau_d}(Y_s - Y_{\mathrm{fv}}^*) \tag{8}$$

$$\frac{\mathrm{d}m_d}{\mathrm{d}t} = -f_4\tau_d^{\frac{1}{3}}(Y_s - Y_{\mathrm{fv}}^*) \tag{9}$$

The droplet variables are normalized using the same reference scales as those used for the gas phase variables. The function f_1 in Eq. (7) represents an empirical correction to the Stokes drag for large droplet Reynolds numbers.[37]

The droplets are assumed lumped, so that there is no temperature variation within each droplet. The factor f_2 in Eq. (8) represents a correlation for the convective heat transfer coefficient based on an empirically corrected Nusselt number.[38] The second term on the right-hand side of Eq. (8) represents the change in the thermal energy because of phase change. The correlation f_3 is a function of an

empirically corrected Sherwood number.[38] For equivalent molecular weights of the gas and the liquid, the vapor mass fraction at the surface of the droplet is proportional to the partial pressure of the vapor. Using the Clausius–Clapeyron relation, the surface mass fraction is described as

$$Y_s = \frac{p_B}{p} \exp\left[\frac{\gamma\lambda}{(\gamma-1)T_B}\left(1-\frac{T_B}{T_d}\right)\right] \tag{10}$$

where T_B is the boiling temperature of the liquid at the pressure p_B. Finally, Eq. (9) governs the rate of mass transfer from the droplet because of phase change that is a function of the fuel vapor mass fraction difference at the droplet surface, the droplet time constant, and the Sherwood number dependent correlation f_4.

For the dilute two-phase flow considered here, it can be assumed that the chemical reaction is in the carrier phase where the fuel vapor and the oxidizer are mixed.[33] Here we consider a second-order and irreversible reaction:

$$F + rO \xrightarrow{K_{fwd}} (1+r)P \tag{11}$$

where F, O, and P represent the fuel vapor, the oxidizer, and the product, respectively. The effects of the heat released by combustion and the phase change energy are accounted for in the description of the absolute enthalpies.

The source/sink terms $\mathcal{S}_m$, $\mathcal{S}_{ui}$, and $\mathcal{S}_e$ appearing in Eqs. (1–4) represent the integrated effects of the droplets mass, momentum, and energy exchange with the carrier phase. These Eulerian variables are calculated from the Lagrangian droplet variables by volume averaging the contributions from all of the individual droplets residing within the cell volume centered around each grid point. The coupling terms are expressed as

$$\mathcal{S}_m = -\frac{1}{\delta\mathcal{V}} \sum^{n_d} \frac{\mathrm{d}m_d}{\mathrm{d}t} \tag{12}$$

$$\mathcal{S}_{ui} = -\frac{1}{\delta\mathcal{V}} \sum^{n_d} \frac{\mathrm{d}}{\mathrm{d}t}(m_d v_i) \tag{13}$$

$$\mathcal{S}_e = -\frac{1}{\delta\mathcal{V}} \sum^{n_d} \left[\frac{\mathrm{d}}{\mathrm{d}t}\left(\frac{1}{2}m_d v_i v_i\right) + \frac{1}{(\gamma-1)M_f^2}\frac{\mathrm{d}}{\mathrm{d}t}(m_d T_d) - \frac{\lambda}{(\gamma-1)M_f^2}\frac{\mathrm{d}m_d}{\mathrm{d}t}\right] \tag{14}$$

Simulations are conducted within the domain $0 \le x_i \le 2\pi$ $(i = 1, 2, 3)$. The reference length L_f is conveniently chosen such that the normalized length of the computational box is 2π. The reference temperature T_f and density ρ_f are set the same as the initial mean temperature and density of the carrier phase, and the reference velocity U_f is found by setting $M_f = 1$. A Fourier spectral collocation method[3] with triply periodic boundary conditions is employed to simulate the transport equation of the carrier phase. The simulations are conducted on a domain discretized by N equally spaced collocation points in each direction. Time advancement for both the Eulerian carrier phase equations and the Lagrangian droplet equations is performed using the second-order-accurate Adams–Bashforth scheme. The magnitudes of the Eulerian gas variables at the droplet locations are determined by a fourth-order Lagrange polynomial interpolation scheme. The turbulence field pertaining to the carrier phase is isotropic. The initial flow for reacting simulations is generated by allowing the droplets to interact as solid particles with a forced stationary flow for more than three eddy turnover times. To emulate the stationary field, a low wavenumber forcing scheme is imposed by adding energy to the large scales of the flow.[32] Once the droplet-laden flow becomes statistically stationary, the time is set to zero and the droplets are allowed to evaporate and react.

Results

The preceding formulation involves a large number of parameters such as the droplet time constant, the mass loading ratio, the initial droplet temperature, the latent heat of evaporation, the boiling temperature, the Damköhler number, the heat release coefficient, and the stoichiometric coefficient. Extensive numerical simulations have been carried out to study the effects of these parameters on various statistics of the reacting flow. Space limitation, however, does not allow us to discuss all of the results in this paper. Therefore, the discussion is limited to the effects of the mass loading ratio (for $\Phi_{m0} = 0.25, 0.5, 1$ with $Ce = 24$) and the heat release coefficient (for $Ce = 8, 16, 24$ with $\Phi_{m0} = 1$) that exhibit somewhat stronger effects on the combustion process. For all of the cases considered here, $Re_f = 600$, $Sc = 0.7$, $\gamma = 1.4$, and $\rho_d = 1000$. Also, $\tau_{d0} = 4$, $\lambda = 2$, $T_B = 5$, $T_{d0} = 1$, $Da = 0.5$, $r = 1$, and p_B is chosen to be the same as the initial pressure of the oxidizer gas. These parameter values do not correspond to any specific application, rather they have been carefully chosen based on previous DNS of single-phase reacting or two-phase nonreacting flows to ensure accuracy of the simulated fields. All of the simulations are performed on 64^3 collocation points using as many as 3.6×10^5 droplets. A typical run (for the case with 3.6×10^5 droplets) requires about 40 h of CPU time on the Cray T90 supercomputer. The results of the simulations are statistically analyzed; in the following, the notation $\langle\,\rangle$ indicates the Eulerian ensemble average and $\langle\langle\,\rangle\rangle$ denotes the Lagrangian average values.

The analysis of the DNS results indicates that the amount of energy added to the system by external forcing is very negligible in comparison to the phase change energy and the heat released by combustion.[32] Therefore, the statistics presented here are not affected by external forcing. The results also indicate that the mean turbulence Mach number is less than 0.12 for all of the cases and the flow is free of shocklets. This is important as a pseudospectral method has been used for simulation of the carrier phase. The turbulence Mach number decreases with the increase of either the heat release coefficient or the mass loading ratio. This is due mainly to the increase of the temperature in the presence of chemical reaction and the decrease of the velocity fluctuations with the increase of the mass loading ratio. The initial carrier phase rms fluctuating velocity, without chemical reaction, is 0.0874, 0.0777, and 0.0667 for $\Phi_{m0} = 0.25$, 0.5, and 1, respectively. The corresponding dissipation rate of the turbulence kinetic energy of the carrier phase is 1.856×10^{-4}, 2.309×10^{-4}, and 3.007×10^{-4}, respectively. These values are calculated by averaging over the stationary period when the droplets are not reacting.

Because the grid resolution for these simulations is somewhat low, various statistics of the flow have been carefully analyzed to ensure that all of the Eulerian fields are accurately resolved. To establish the grid independency of the results, the case with the highest mass loading ratio and heat release coefficient ($\Phi_{m0} = 1$, $Ce = 24$) has been repeated using 48^3 collocation points. To provide a direct comparison between the results obtained from the two different grid resolutions, it is necessary to keep all the time and length scales involved in the problem the same. This is only possible by using the same parameter values, including $Re_f = 600$, for both simulations. Figure 1 shows that the temporal variations of the average mass of the droplets and their mean temperature from the two simulations are in very close agreement. Comparison of other statistics (not shown)

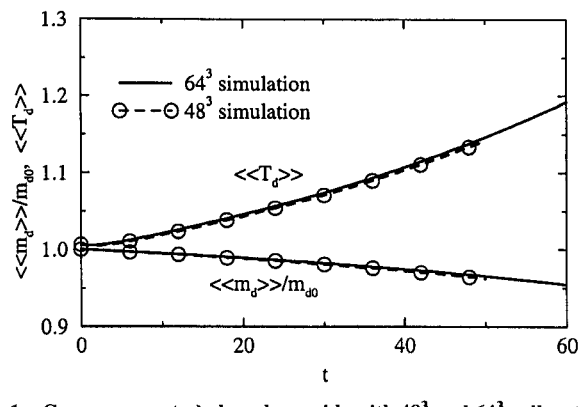

Fig. 1 Convergence study based on grids with 48^3 and 64^3 collocation points.

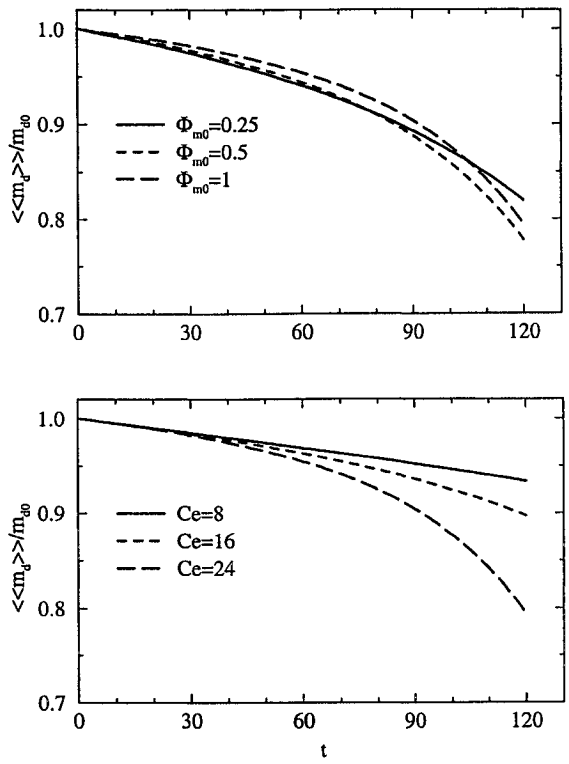

Fig. 2 Temporal variations of the Lagrangian average mass of the droplets normalized with its initial value.

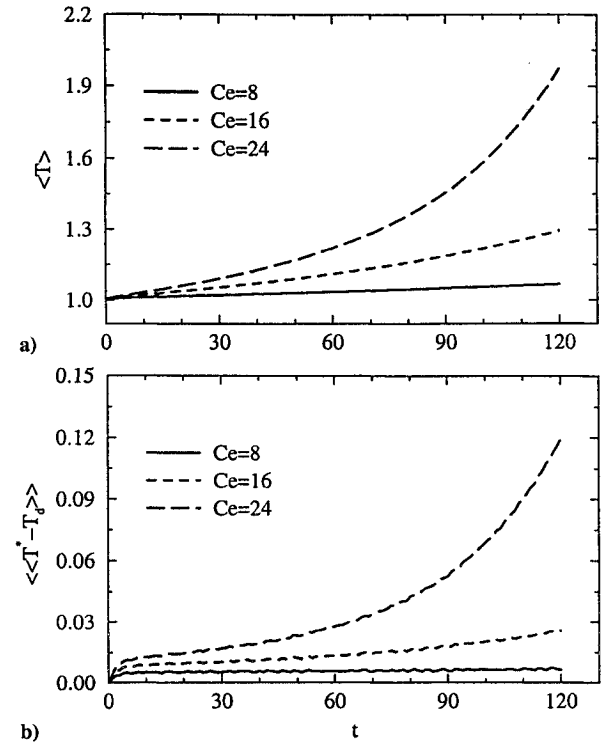

Fig. 3 Temporal variations of a) the mean temperature of the carrier phase and b) the Lagrangian mean temperature difference.

from the two simulations also indicated close agreements. The 48^3 simulation was terminated after about three eddy turnover times as Re_f used for this simulation is relatively high.

The temporal variation of the Lagrangian average droplet mass (normalized with its initial value) is shown in Fig. 2. A close inspection of this figure reveals that, during the initial times, the normalized mass decreases faster for smaller mass loading ratios. This is in qualitative agreement with the results of Mashayek[32] for evaporating (not reacting) droplets. In early times, combustion is not very effective as the amount of the fuel vapor is small. As the chemical reaction proceeds, more heat is released and the rate of evaporation increases, which in turn results in higher rates of reaction. As a result, at longer times the normalized mass of the droplets decreases faster at higher mass loading ratios. For the same reason, i.e., low reaction rate, the variation of the heat release coefficient does not significantly affect the evaporation rate during the early stages. As expected, for longer times the increase of the heat release coefficient results in the increase of the heat generated by combustion, thus increasing the evaporation rate.

The heat released by reaction causes the temperature of both phases to rise, as illustrated in Fig. 3a for the carrier phase. However, it must be noted that a portion of the heat is utilized to account for the latent heat of evaporation and does not contribute to the change of the sensible heat that is exhibited by a rise in the temperature. This is more evident during the early stages as the fuel vapor mass fraction is small and so is the heat released by combustion. For small values of the heat release coefficient the rate of evaporation is small and the rate of temperature increase remains small for all times (Fig. 3a). For large values of the heat release coefficient, however, more vapor is generated and the reaction rate increases. Therefore, a large amount of heat is generated although only a small fraction is consumed for the latent heat of evaporation. This results in significant increase in the mean temperature at long times. The increase of the mass loading ratio enhances the amount of the fuel vapor and increasingly raises the temperature (not shown). Figure 3b shows that the difference in the temperatures of the two phases also increases with time for high heat release values. This increases the heat transfer from the carrier phase to the droplets and results in higher evaporation rates. It is interesting to note in Fig. 3b that for $Ce = 8$ the mean temperature difference remains nearly stationary in time despite the increase in the temperatures of both phases.

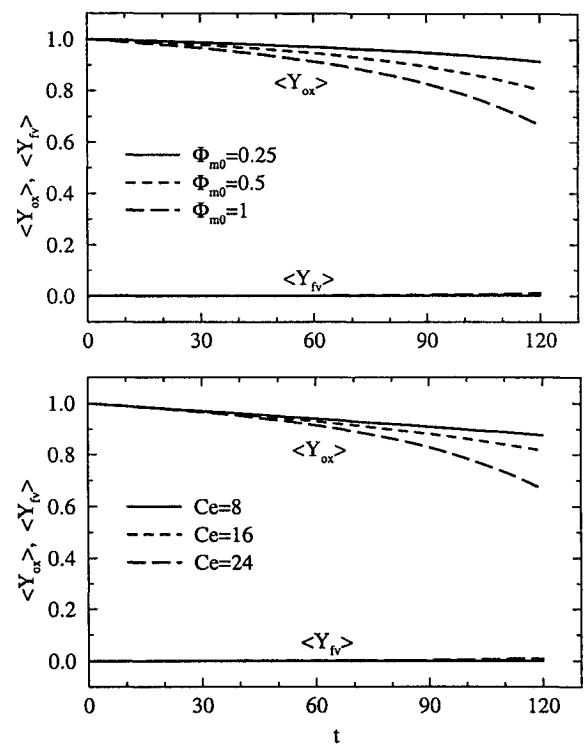

Fig. 4 Temporal variations of the mean mass fractions of the oxidizer and the fuel vapor.

The discussion on the rate of evaporation (cf. Fig. 2) does not identify the temporal behavior of the fuel vapor mass fraction because part of the generated vapor is continuously consumed by combustion. In fact, as shown in Fig. 4, the mean vapor mass fraction remains close to zero throughout the simulations. This implies that the fuel vapor participates in the chemical reaction almost immediately after its production. The increase of the heat release coefficient and/or the mass loading ratio increases the rate of evaporation. This may result in local accumulation of the vapor without access to enough oxidizer. This is observed by close inspection of Fig. 4, which shows

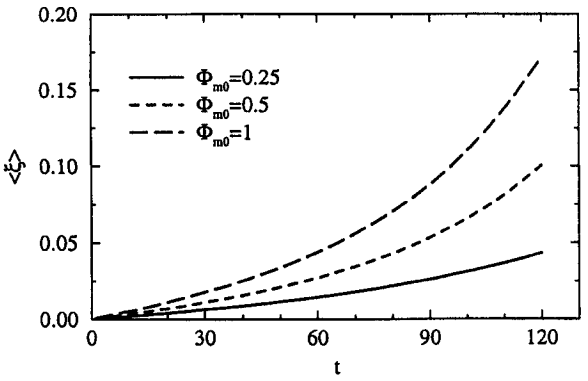

Fig. 5 Temporal variations of the mean mixture fraction.

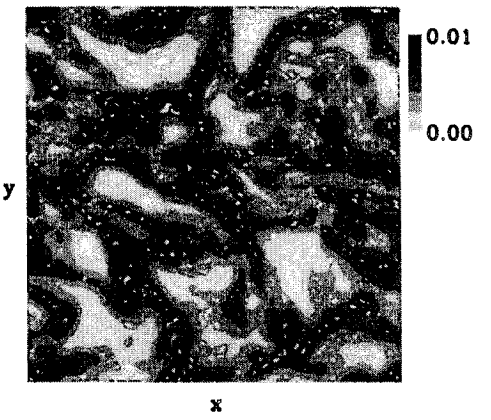

Fig. 6 Instantaneous contours of the reaction rate in a typical x–y plane for the case with $\Phi_{m0} = 1$ and $Ce = 24$ at $t = 100$.

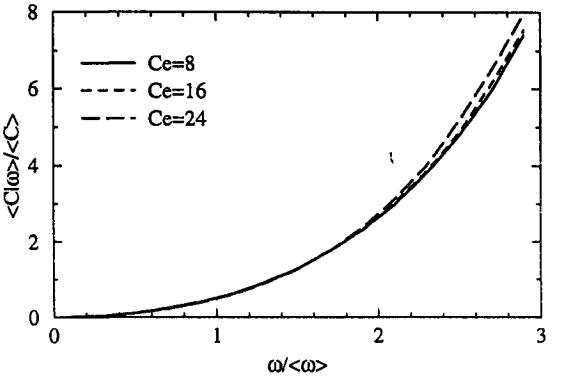

Fig. 7 Variations of the expected value of the droplet concentration conditioned on the reaction rate.

that the mean fuel vapor mass fraction starts to deviate from zero at long times. The decrease of the mass fraction of the oxidizer at long times (Fig. 4) is also responsible for this phenomenon.

A convenient approach usually adopted to analyze a reaction is via the concept of mixture fraction defined as[39]

$$\xi = \frac{Y_{fv} - (1/r)Y_{ox} + 1/r}{1 + 1/r} \tag{15}$$

In single-phase flows, without any source of fuel or oxidizer, ξ behaves like a conserved scalar. For the present case, however, ξ is not conserved and increases with time as shown in Fig. 5. To analyze the behavior observed in the figure, the transport equation for ξ is derived using Eqs. (1), (4), and (5):

$$\frac{\partial}{\partial t}(\rho\xi) + \frac{\partial}{\partial x_j}(\rho\xi u_j) = \frac{1}{ScRe_f}\frac{\partial^2\xi}{\partial x_j \partial x_j} + \mathcal{S}_m \tag{16}$$

which resembles the equation for a conserved scalar except for the droplet mass source term. For evaporating droplets, this term is always positive and results in the increase of ξ. For homogeneous flows, a relationship between the mean value of ξ and the mean carrier phase density may be obtained by averaging Eq. (16). After some algebraic manipulations and by assuming that $\langle\rho\xi\rangle \simeq \langle\rho\rangle\langle\xi\rangle$ the following relation is obtained:

$$\langle\xi\rangle \simeq \frac{\langle\rho\rangle - \langle\rho_0\rangle}{\langle\rho\rangle} \tag{17}$$

where ρ_0 is the initial value of the carrier phase density. Equation (17) is in excellent agreement with the results of the simulations.

When analyzing the DNS results, special attention must be paid to various mechanisms influencing the mixing of the fuel vapor and the oxidizer. The extensive previous studies conducted on single-phase turbulent reacting flows have revealed the important role of turbulence mixing in enhancing the rate of reaction. In two-phase reacting flows, the dispersion of the droplets may also be considered as an effective mechanism for improving and/or controlling the mixing process. The most important issue in this consideration is the preferential distribution of the droplets.[18,28] Figure 6 portrays the contours of the reaction rate in a typical x–y ($x \equiv x_1$ and $y \equiv x_2$) plane; similar behavior was observed in other planes. It is clear that the reaction zone is composed of local intense areas surrounded by regions with low reaction rate. A comparison with the contours of the droplet concentration (not shown) revealed that the regions of high reaction rate closely correspond to areas with high droplet concentration. For the present simulations, a considerable portion of the domain is free of droplets, mainly because of the preferential distribution of the droplets in high strain rate regions of the flow.

To quantify the correlation between the droplet concentration and the reaction rate, in Fig. 7 we consider the variations of $\langle C \mid \omega\rangle/\langle C\rangle$ with $\omega/\langle\omega\rangle$ for different values of the heat release coefficient. The results in Fig. 7 confirm that the droplets are mostly concentrated in the regions of the flow with high reaction rates. This may be explained by considering that the droplets are the source for the fuel vapor; therefore there is a higher probability for having higher reaction rates in the vicinity of the droplets. However, it could also be (at least partially) because of the effects of reaction on the vorticity field that play a significant role in the preferential distribution of the droplets. This latter scenario has not yet been explored and demands more future elaboration.

Conclusion

Results obtained via numerical simulation are used to investigate some issues of relevance to dispersion and polydispersity of evaporating and reacting droplets in forced isotropic compressible turbulence at low Mach numbers. Although we have been able to consider a reasonably wide parameter range, because of space limitation we only discuss the effects of the mass loading ratio and the heat release coefficient here. The decrease of the mass loading ratio results in a faster decrease of the relative mass (normalized with its initial value) of the droplets during the initial times; an opposite trend is observed at long times. The increase of the heat release coefficient monotonically increases the rate of evaporation at all times. An analysis of the results indicates that evaporation plays a significant role during the early stages of combustion for all of the cases. At longer times, and for larger values of the heat release coefficient, the temperature of the mixture increases to large values that (by increasing the heat transfer between the phases) results in large evaporation rates. The fuel vapor participates in chemical reaction almost immediately after its production and a strong correlation is observed between the droplet concentration and the reaction rate. The results also show the preferential distribution of the droplets, which plays a significant role in the structure of the reaction zone.

Acknowledgments

The support for this work was provided by Donors of the Petroleum Research Fund Grant 33044-G9, administered by the American Chemical Society, and Grant CTS-9874655 from the National Science Foundation. Computational resources were provided by the San Diego Supercomputing Center and the College of Engineering Computer Facility at the University of Hawaii at Manoa.

References

[1]Faeth, G. M., "Mixing, Transport and Combustion in Sprays," *Progress in Energy and Combustion Sciences*, Vol. 13, 1987, pp. 293–345.

[2]Givi, P., "Model Free Simulations of Turbulent Reactive Flows," *Progress in Energy and Combustion Sciences*, Vol. 15, 1989, pp. 1–107.

[3]Givi, P., "Spectral and Random Vortex Methods in Turbulent Reacting Flows," *Turbulent Reacting Flows*, edited by P. A. Libby, and F. A. Williams, Academic, London, 1994, pp. 475–572.

[4]Taylor, G. I., "Diffusion by Continuous Movements," *Proceedings of the London Mathematics Society*, Vol. 20, 1921, pp. 196–211.

[5]Hill, J. C., "Simulation of Chemical Reaction in a Turbulent Flow," *Proceedings of the Second R. F. Ruth Chemical Engineering Research Symposium*, Ames, IA, 1979, pp. 27–53.

[6]McMurtry, P. A., and Givi, P., "Direct Numerical Simulations of Mixing and Reaction in a Nonpremixed Homogeneous Turbulent Flow," *Combustion and Flame*, Vol. 77, 1989, pp. 171–185.

[7]Gao, F., and O'Brien, E. E., "Direct Numerical Simulations of Reacting Flows in Homogeneous Turbulence," *AIChE Journal*, Vol. 37, No. 10, 1991, pp. 1459–1470.

[8]Nomura, K. K., and Elghobashi, S. E., "Mixing Characteristics of an Inhomogeneous Scalar in Isotropic and Homogeneous Sheared Turbulence," *Physics of Fluids A*, Vol. 4, March 1992, pp. 606–625.

[9]Leonard, A. D., and Hill, J. C., "Mixing and Chemical Reaction in Sheared and Nonsheared Homogeneous Turbulence," *Fluid Dynamics Research*, Vol. 10, 1992, pp. 273–297.

[10]Swaminathan, N., Mahalingam, S., and Kerr, R. M., "Structure of Nonpremixed Reaction Zones in Numerical Isotropic Turbulence," *Theoretical and Computational Fluid Dynamics*, Vol. 8, No. 3, 1996, pp. 201–218.

[11]Jaberi, F. A., Miller, R. S., Mashayek, F., and Givi, P., "Differential Diffusion in Binary Scalar Mixing and Reaction," *Combustion and Flame*, Vol. 109, 1997, pp. 561–577.

[12]McMurtry, P. A., Jou, W.-H., Riley, J. J., and Metcalfe, R. W., "Direct Numerical Simulations of a Reacting Mixing Layer with Chemical Heat Release," *AIAA Journal*, Vol. 24, No. 6, 1986, pp. 962–970.

[13]Menon, S., and Fernando, E., "A Numerical Study of Mixing and Chemical Heat Release in Supersonic Mixing Layers," AIAA Paper 90-0152, Jan. 1990.

[14]Balakrishnan, G., Sarkar, S., and Williams, F. A., "Direct Numerical Simulation of Diffusion Flames with Large Heat Release in Compressible Homogeneous Turbulence," AIAA Paper 95-2375, 1995.

[15]Riley, J. J., and Patterson, G. S., "Diffusion Experiments with Numerically Integrated Isotropic Turbulence," *Physics of Fluids*, Vol. 17, No. 2, 1974, pp. 292–297.

[16]Squires, K. D., and Eaton, J. K., "Particle Response and Turbulence Modification in Isotropic Turbulence," *Physics of Fluids*, Vol. 2, No. 7, 1990, pp. 1191–1203.

[17]Elghobashi, S., and Truesdell, G. C., "Direct Simulation of Particle Dispersion in a Decaying Isotropic Turbulence," *Journal of Fluid Mechanics*, Vol. 242, 1992, pp. 655–700.

[18]Wang, L.-P., and Maxey, M. R., "Settling Velocity and Concentration Distribution of Heavy Particles in Isotropic Turbulence," *Journal of Fluid Mechanics*, Vol. 256, 1993, pp. 27–68.

[19]Mashayek, F., Taulbee, D. B., and Givi, P., "Modeling and Simulation of Two-Phase Turbulent Flow," *Propulsion Combustion: Fuels to Emissions*, edited G. D. Roy, Taylor and Francis, Washington, DC, 1998, pp. 241–280.

[20]McLaughlin, J. B., "Aerosol Particle Deposition in Numerically Simulated Channel Flow," *Physics of Fluids*, Vol. 1, No. 7, 1989, pp. 1211–1224.

[21]Ounis, H., Ahmadi, G., and McLaughlin, J. B., "Dispersion and Deposition of Brownian Particles from Point Sources in a Simulated Turbulent Channel Flow," *Journal of Colloid and Interface Science*, Vol. 147, No. 1, 1991, pp. 233–250.

[22]Brooke, J. W., Hanratty, T. J., and McLaughlin, J. B., "Free-Flight Mixing and Deposition of Aerosols," *Physics of Fluids*, Vol. 6, No. 10, 1994, pp. 3404–3415.

[23]Chen, M., and McLaughlin, J. B., "A New Correlation for the Aerosol Deposition Rate in Vertical Ducts," *Journal of Colloid and Interface Science*, Vol. 169, 1995, pp. 437–455.

[24]Rouson, D. W. I., Eaton, J. K., and Abrahamson, S. D., "A Direct Numerical Simulation of a Particle-Laden Turbulent Channel Flow," Dept. of Mechanical Engineering, Rept. TSD-101, Stanford Univ., Stanford, CA, 1997.

[25]Miller, R. S., Harstad, K., and Bellan, J., "Evaluation of Equilibrium and Non-Equilibrium Evaporation Models for Many-Droplet Gas-Liquid Flow Simulations," *International Journal of Multiphase Flow*, Vol. 24, No. 6, 1998, pp. 1025–1055.

[26]Miller, R. S., and Bellan, N. J., "Direct Numerical Simulation of a Confined Three-Dimensional Gas Mixing Layer with One Evaporating Hydrocarbon-Droplet Laden Stream," *Journal of Fluid Mechanics*, Vol. 384, 1999, pp. 293–338.

[27]McLaughlin, J. B., "Numerical Computation of Particles-Turbulence Interaction," *International Journal of Multiphase Flow, Supplementary*, Vol. 20, 1994, pp. 211–232.

[28]Eaton, J. K., and Fessler, J. R., "Preferential Concentration of Particles by Turbulence," *International Journal of Multiphase Flow, Supplementary*, Vol. 20, 1994, pp. 169–209.

[29]Crowe, C., Troutt, T., and Chung, J., "Numerical Models for Two-Phase Turbulent Flows," *Annual Review of Fluid Mechanics*, Vol. 28, 1996, pp. 11–43.

[30]Mashayek, F., Jaberi, F. A., Miller, R. S., and Givi, P., "Dispersion and Polydispersity of Droplets in Stationary Isotropic Turbulence," *International Journal of Multiphase Flow*, Vol. 23, No. 2, 1997, pp. 337–355.

[31]Mashayek, F., "Droplet-Turbulence Interactions in Low-Mach-Number Homogeneous Shear Two-Phase Flows," *Journal of Fluid Mechanics*, Vol. 376, 1998, pp. 163–203.

[32]Mashayek, F., "Direct Numerical Simulations of Evaporating Droplet Dispersion in Forced Low-Mach-Number Turbulence," *International Journal of Heat and Mass Transfer*, Vol. 41, No. 17, 1998, pp. 2601–2617.

[33]Chiu, H. H., and Liu, T. M., "Group Combustion of Liquid Droplets," *Combustion Science and Technology*, Vol. 17, 1977, pp. 127–142.

[34]Mashayek, F., "Numerical Simulation of Heterogeneous Flow with Homogeneous Reaction," AIAA Paper 99-0204, Jan. 1999.

[35]Turns, S. R., *An Introduction to Combustion: Concepts and Applications*, McGraw–Hill, New York, 1996, Chap. 7.

[36]Crowe, C. T., Sharma, M. P., and Stock, D. E., "The Particle-Source in Cell (PSI-Cell) Model for Gas-Droplet Flows," *Journal of Fluids Engineering*, Vol. 6, June 1977, pp. 325–332.

[37]Wallis, G. B., *One Dimensional Two Phase Flow*, McGraw–Hill, New York, 1969.

[38]Bird, R. B., Stewart, W. E., and Lightfoot, E. N., *Transport Phenomena*, Wiley, New York, 1960.

[39]Bilger, R. W., "Turbulent Flows with Nonpremixed Reactants," *Turbulent Reacting Flows*, edited by P. A. Libby and F. A. Williams, Vol. 44, Topics in Applied Physics, Springer–Verlag, Heidelberg, Germany, 1980, pp. 65–113.

P. Givi
Associate Editor